Electronic Supplementary Information for

Cationic-Anionic Redox Couple Gradient to Immunize Against Irreversible Processes of Li-rich Layered Oxides

Yi Pei [a,b†], Shuang Li [b,c†], Qing Chen [b†], Ruilin Liang [b], Matthew Li [b], Rui Gao [b], Dezhang Ren [b], Ya-Ping Deng [b], Huile Jin [a], Shun Wang [a*], Dong Su [d], Yongfeng Hu [e], Zhongwei Chen [b*]

[a] Nano-materials & Chemistry Key Laboratory, Institute of New Materials and Industrial Technologies, Wenzhou University, Wenzhou, Zhejiang, 325035, China

[b] Department of Chemical Engineering, Waterloo Institute for Nanotechnology, University of Waterloo, Waterloo, Ontario, N2L 3G1, Canada

[c] Center for Functional Nanomaterials, Brookhaven National Laboratory, Upton, NY, 11973, USA.

[d] Beijing National Laboratory for Condensed Matter Physics, Institute of Physics, Chinese Academy of Sciences, Beijing, 100190, China.

[e] Canadian Light Source, University of Saskatchewan, Saskatoon, Saskatchewan S7N 0X4, Canada

[†] These authors contributed equally to this work.

[*] Corresponding Authors. E-mail: shunwang@wzu.edu.cn (S. Wang), zhwchen@uwaterloo.ca (Z.W. Chen)

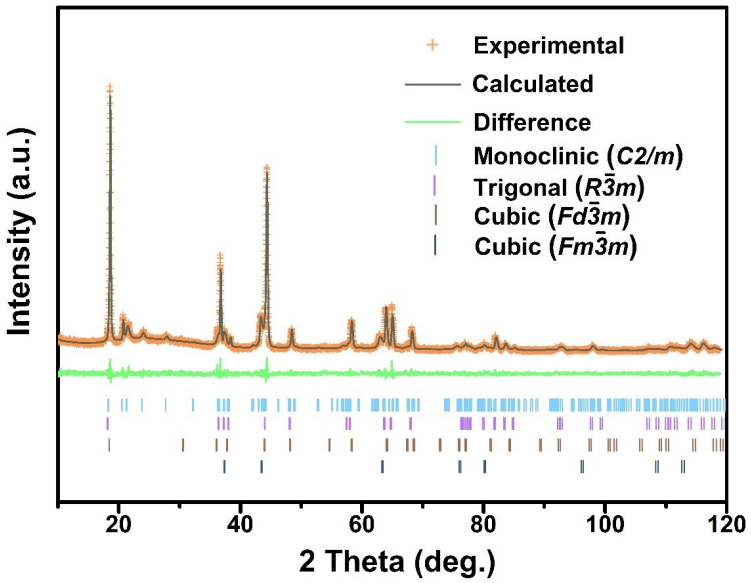

Fig. S1. XRD and corresponding Rietveld refinement pattern of LLO-FC.

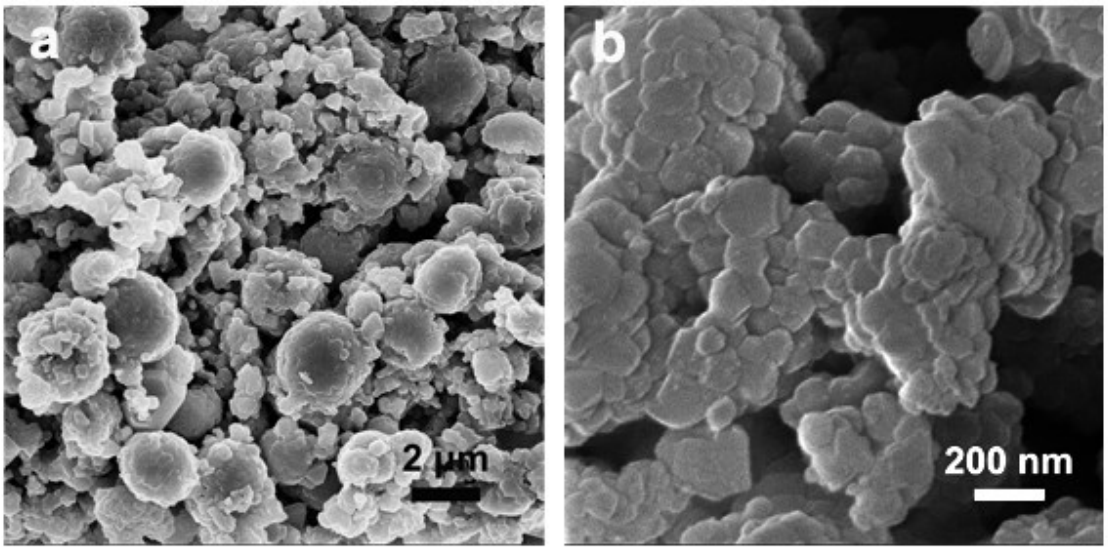

Fig. S2. SEM images of $Li_{1.2}Ni_{0.2}Mn_{0.6}O_2$ with/without F doping. (a) LLO-CP, (b) LLO-FC.

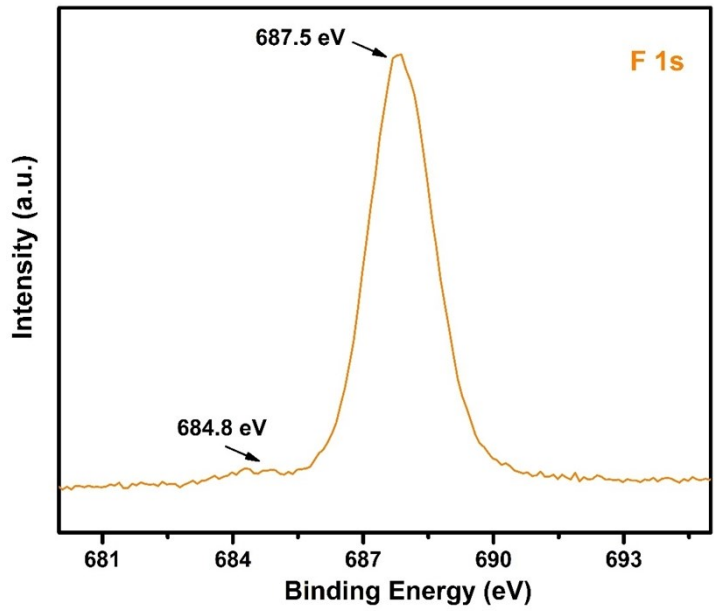

Fig. S3. High resolution F 1s XPS spectrum of LLO-FP.

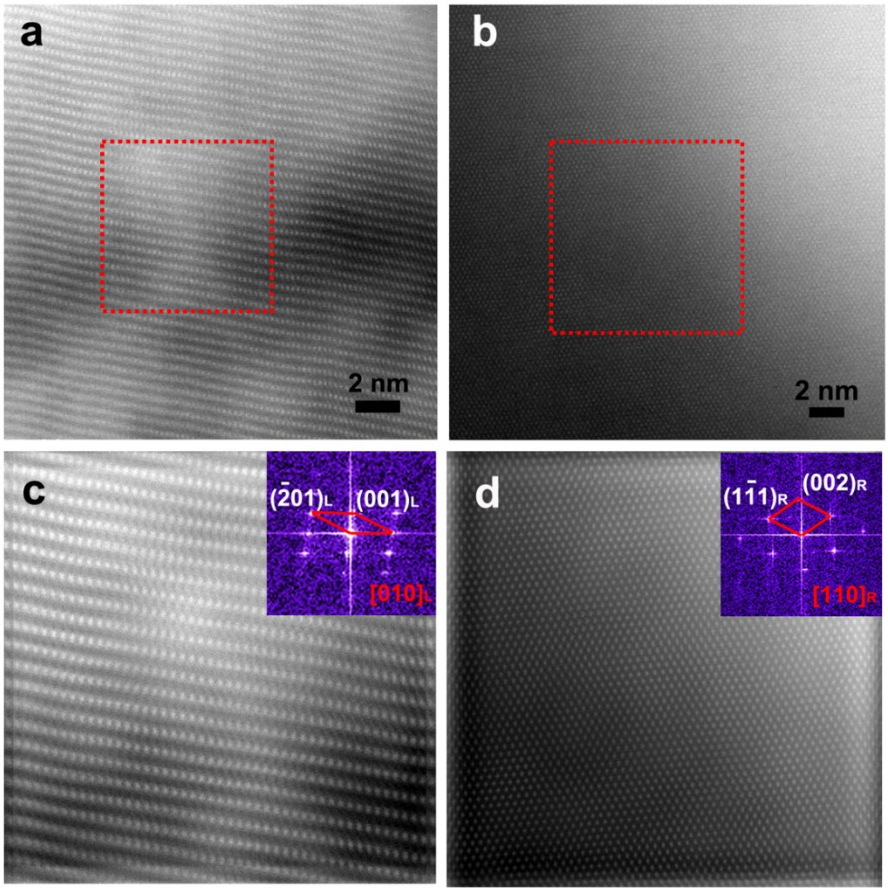

Fig. S4. Atomic configuration of LLO-FC. (a, b) HAADF/STEM images of LLO-FC in the region of layered structure (a) and rock-salt structure (b). (c,d) FFT patterns and FFT filtered images of layered structure and rock-salt structure (d) corresponding to the red dash square in (a) and (b), respectively. The FFT patterns were shown as insets. The FFT pattern in (c) could be indexed to the [010] zone axis of Li-rich layered structure (Li_2MnO_3, *C2/m*) and the FFT pattern in (d) could be indexed to the [110] zone axis of rock-salt structure ($Li_xNi_{1-x}O$, *Fm***Error!***m*)

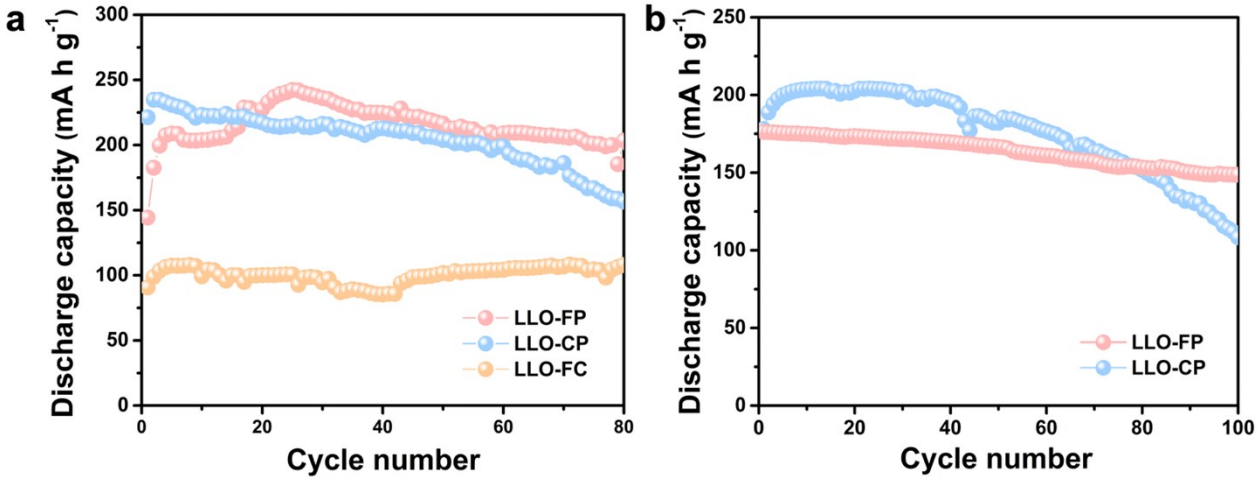

Fig. S5. (a) 0.2 C and (b) 1C cycling performance of LLO with and without Fluoride ion doping.

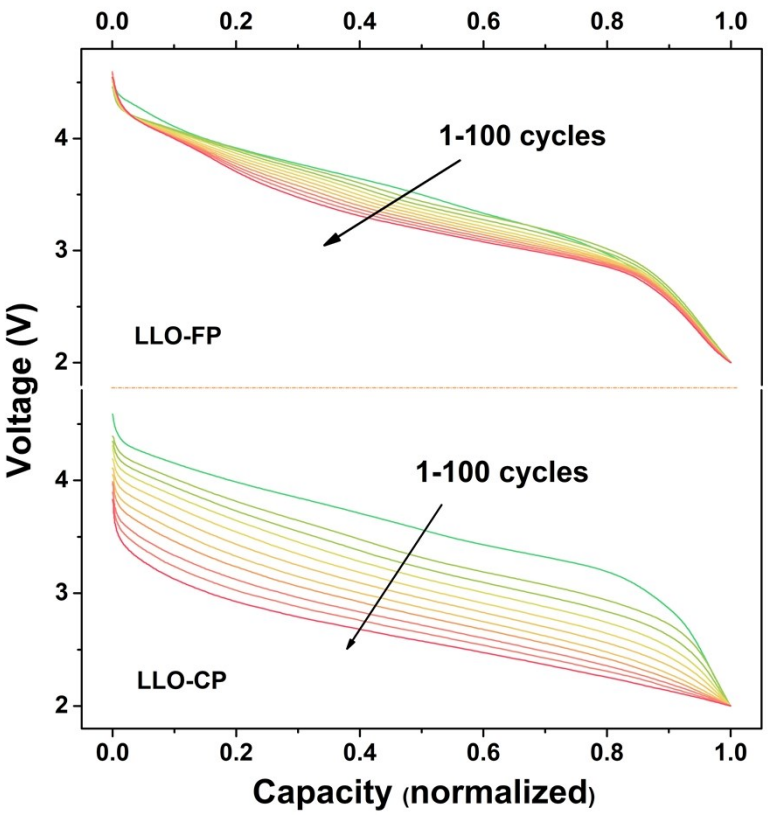

Fig. S6. Normalized galvanostatic discharge profiles of LLO-FP and LLO-CP at 0.5C from 1 to 100 cycles.

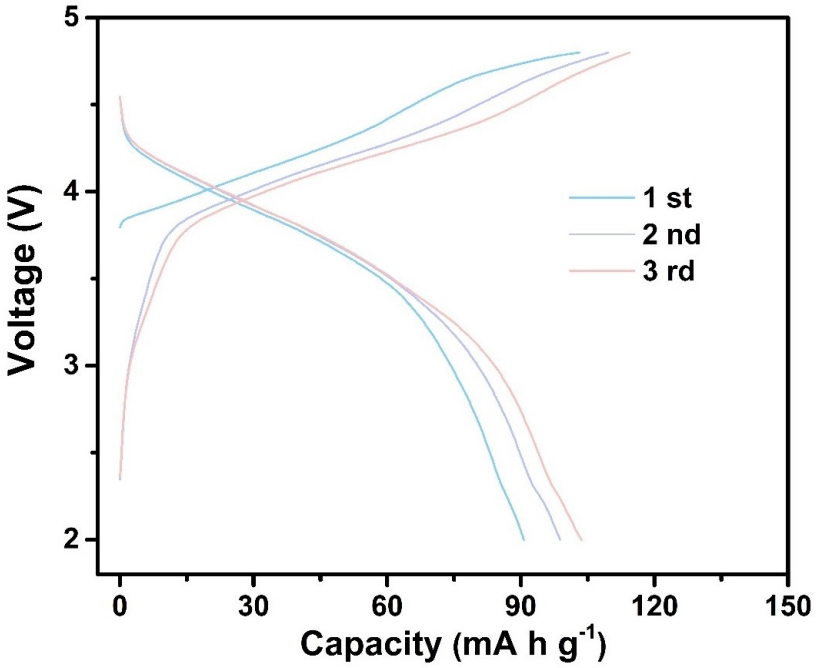

Fig. S7. 0.2C charge-discharge profiles of LLO-FC in the first three cycles.

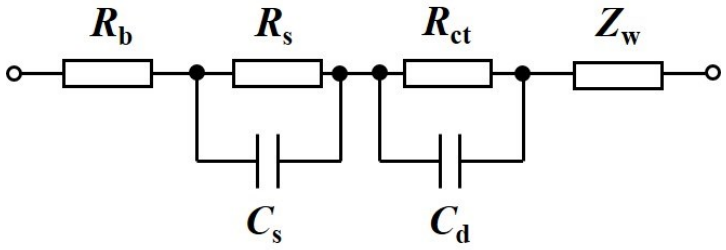

Fig. S8. Equivalent circuit adapted to fit the electrochemical impedance spectra. R_b representing the bulk resistance, R_s is referred to the surface film resistance, R_{ct} is referred to the charge-transfer resistance, C_s is the surface film capacitance, C_d is the double layer capacitance, and Z_w representing the Warburg impedance associated with Li^+ diffusion in the material particles.

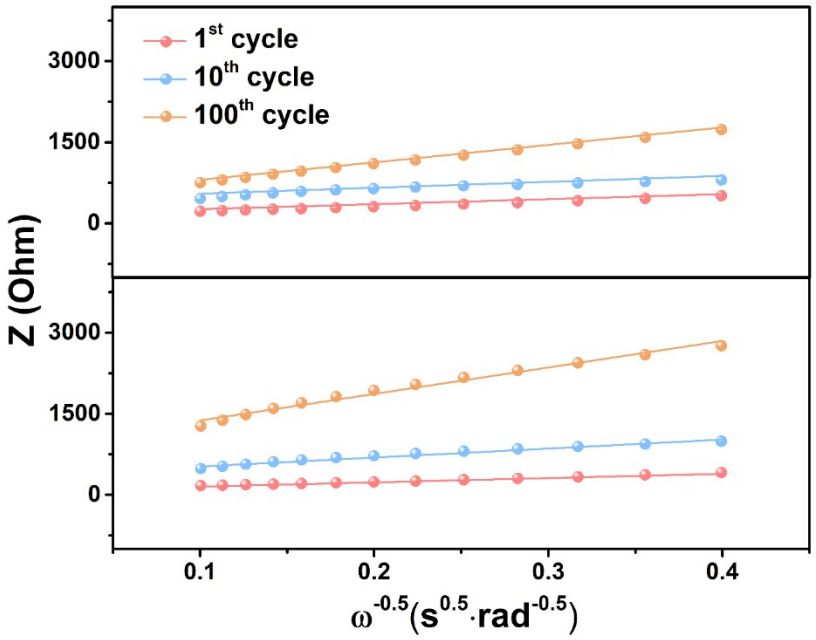

Fig. S9. Z_{re} *vs.* $\omega^{-0.5}$ plots of LLO-CP and LLO-FP in the low-frequency region.

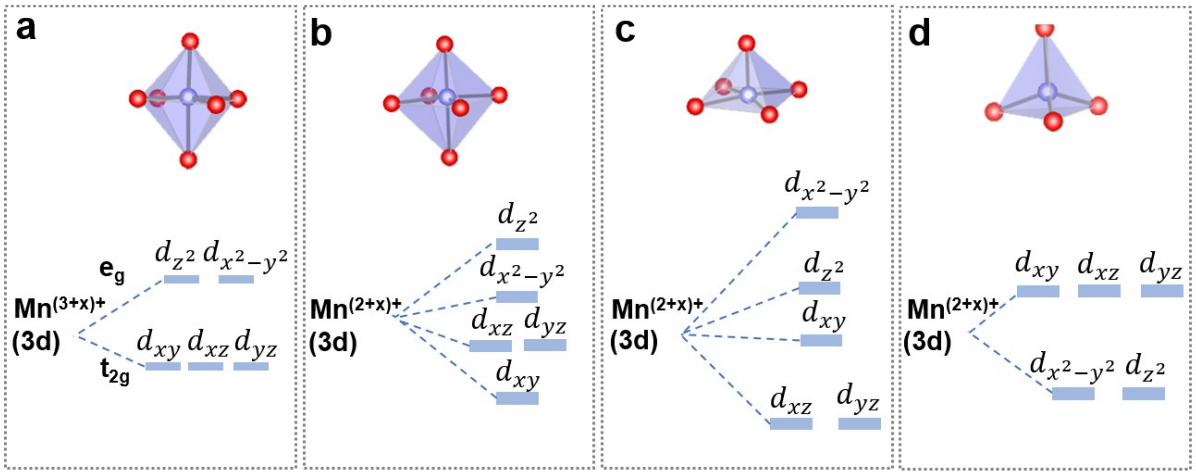

Fig. S10. (a-d) the atomic and electronic configurations of MnO_6 octahedral ligand in LLO (a), compressed MnO_6 octahedral ligand effected by Jahn-Teller effect (b), MnO_5 square pyramidal after the formation of oxygen vacancy (c) and MnO_4 tetrahedral ligand (d) induced by formation of oxygen vacancy.

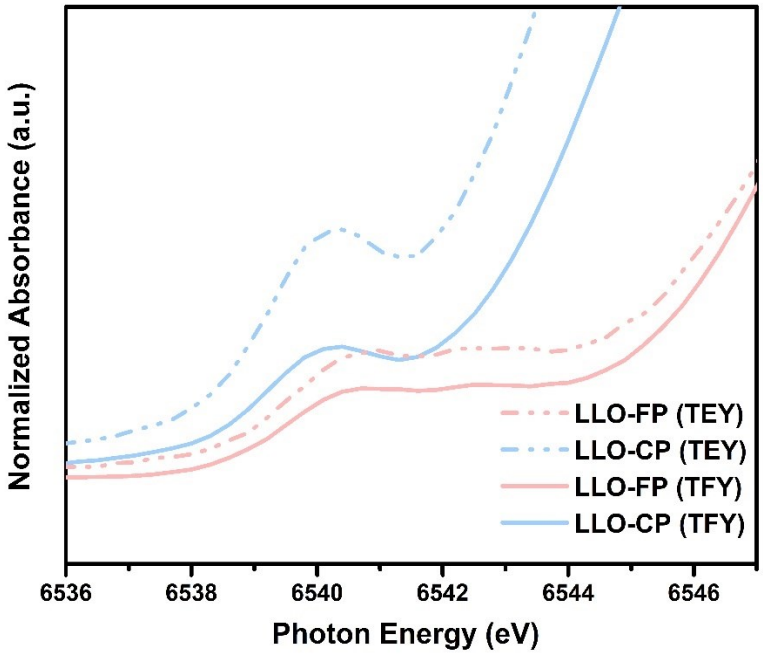

Fig. S11. Enlarged pre-edge region in Mn K-edge spectra of LLO-CP and LLO-FP.

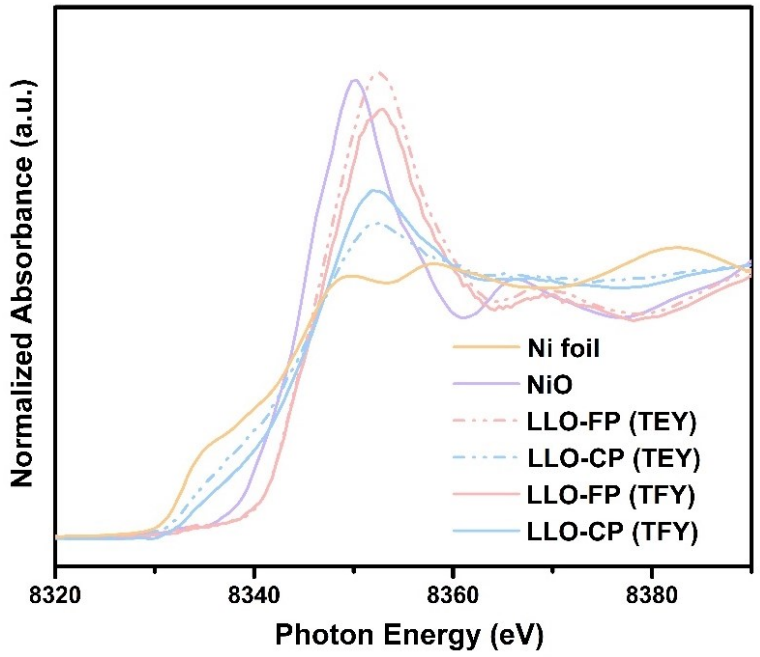

Fig. S12. Normalized XANES Ni K edge spectra of of LLO-CP and LLO-FP electrodes after they were operated for 100 cycles. The valence states of Ni were determined by comparison against spectra of pure-phase Ni and NiO, and the spectra obtained with TEY and TFY modes

were shown by dash and solid line, respectively.

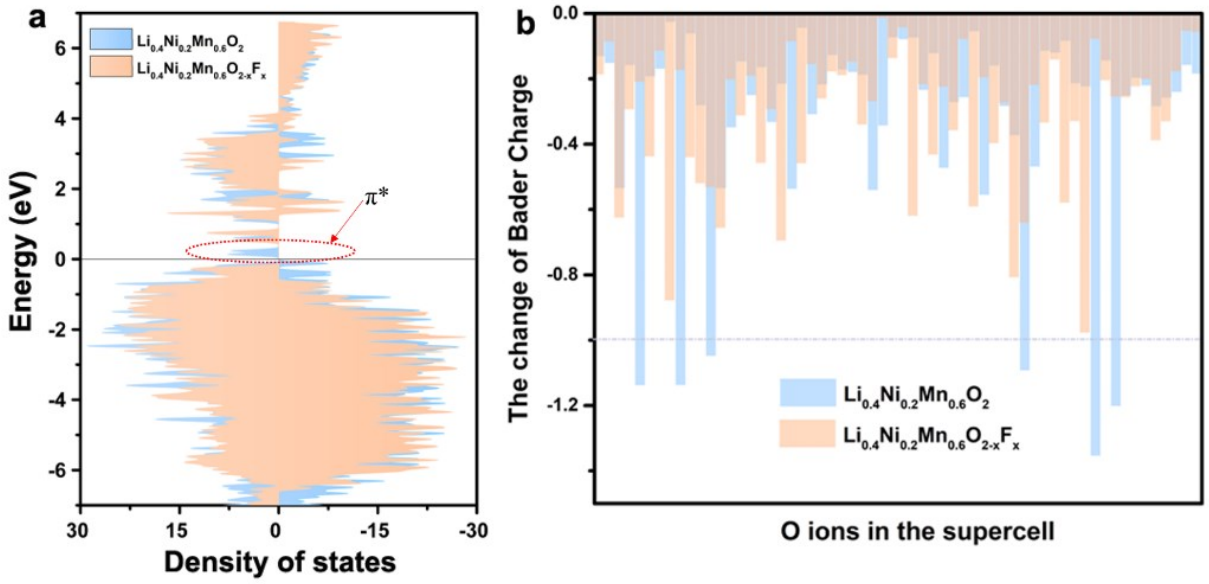

Fig. S13. (a) Partial density of states (PDOS) of O ions in delithiated structures and (b) the change of Bader charge upon delithiation. The empty π* antibonding state in $Li_{0.4}Ni_{0.2}Mn_{0.6}O_2$ was marked by red dash cycle. The negative value in Bader analysis indicated the loss of electrons upon delithiation.

Table S1. XRD Rietveld refinement results of $Li_{1.2}Ni_{0.2}Mn_{0.6}O_2$ before and after F doping.

Sample	Lattice parameter (Å)		$I_{(003)}/I_{(104)}$	Li/Ni interlayer mixing % (Ni_{3b}/ Ni_{total})	R_{wp}	R_p
	a	*c*				
LLO-FP	2.874(0)	14.358(1)	0.84	9.1	9.31	7.46
LLO-CP	2.865(5)	14.347(7)	1.42	2.5	7.89	6.51
LLO-FC	2.877(6)	14.344(0)	1.32	3.1	7.17	6.16

Table S2. Relative concentration of F and O in LLO-FP obtained from XPS

	F	O
Relative concentration (%)	22.4%	77.6%

Table S3. R_s, R_{ct} and D_{Li} values of LLO-CP and LLO-FP after 1, 10 and 100 complete charge/discharge cycles at 0.5 C.

Samples	$R_s(\Omega)$			$R_{ct}(\Omega)$			D_{Li} ($cm^2\ s^{-1}$)		
	1st cycle	10th cycle	100th cycle	1st cycle	10th cycle	100th cycle	1st cycle	10th cycle	100th cycle
LLO-CP	20.46	37.13	32.39	112.9	554.4	951.3	2.99×10^{-14}	6.79×10^{-15}	7.78×10^{-16}
LLO-FP	11.46	34.11	67.72	185.1	354.9	537	2.11×10^{-14}	1.54×10^{-14}	1.76×10^{-15}